The Pure Rotational Spectra of AuCl and AuBr

Corey J. Evans and Michael C. L. Gerry

Department of Chemistry, The University of British Columbia, 2036 Main Mall, Vancouver, British Columbia, Canada V6T 1Z1

The pure rotational spectra of AuCl and AuBr have been measured in the $v = 0$ and 1 (also for $v = 2$ for Au^{35}Cl) vibrational states in the 5–22 GHz spectral region using a cavity pulsed-jet Fourier transform microwave spectrometer. The molecules were prepared by ablating Au metal in the presence of Cl$_2$ or Br$_2$ entrained in the Ar or Ne backing gas of the jet. The equilibrium internuclear distances r_e have been determined along with estimates of the harmonic vibration frequencies and the dissociation energies. The ionic characters of the AuCl and AuBr bonds have been estimated from the halogen nuclear quadrupole-coupling constants to be $i_c \sim 38\%$. The gold nuclear quadrupole coupling constants change appreciably from AuF to AuCl to AuBr (including a sign change), indicating substantial differences in their electronic structures at Au; these variations could not be accounted for with a simple Townes–Dailey calculation. © 2000 Academic Press

INTRODUCTION

Interest in relativistic effects has recently led to many theoretical studies on diatomic gold compounds (*1–13*). The pronounced local maximum contraction of the $6s$ shell in gold makes it a unique element for which to study such effects (*14, 15*). Experimental studies on Au(I) species and their electronic structures have thus far been limited to investigations on solids using NQR (*16*) and Mössbauer spectroscopic techniques (*17*). The results obtained have led to some debate on whether the Au hybridization in these species is predominantly *sd* or *sp* in character (*17a, 17c, 18*).

Fourier transform microwave (FTMW) spectroscopy is ideal for the analysis of hyperfine interactions in such molecules. In this laboratory we have studied several transition metal monohalides using a pulsed-cavity FTMW spectrometer (*19–21*). The determined hyperfine constants have allowed the electronic structures of these molecules to be probed and have helped in gaining some understanding of the nature of bonding of transition metals. Recently we measured and assigned the pure rotational spectrum of AuF (*22*). To help improve the understanding of the bonding in Au(I) monohalides, we have extended our studies to gold(I) monochloride (AuCl) and gold(I) monobromide (AuBr).

AuCl was first observed spectroscopically in 1928 by Ferguson (*23*), who reported electronic transitions of Au^{35}Cl and Au^{37}Cl in the visible region. Several vibronic bands were observed and attributed to the *A–X* and *B–X* electronic transitions. Recently O'Brien *et al.* (*24*) reinvestigated these bands at high resolution ($A\Omega = 1–X^1\Sigma^+$ and $B\Omega = 0^+–X^1\Sigma^+$ electronic states) and determined equilibrium constants for the Au^{35}Cl isotopomer. No hyperfine structure for the ^{197}Au or ^{35}Cl nuclei was observed. Several theoretical studies have been carried out on the electronic ground state of AuCl (*1–5, 7, 9,*

12), giving estimates of various equilibrium constants. To our knowledge, AuBr has not been studied spectroscopically in the gas phase before. A theoretical study by Schwerdtfeger *et al.* (*5*) listed spectroscopic constants for a number of diatomic gold species, including AuBr.

In this paper we report the first measurements of the pure rotational spectra of AuCl and AuBr. Rotational and centrifugal distortion constants have been determined and have been used to evaluate the equilibrium bond distances, r_e, and harmonic frequencies and dissociation energies. The determined hyperfine constants have been used to investigate the nature of the bonding in gold monohalides.

EXPERIMENTAL PROCEDURE

The pure rotational spectra of AuCl and AuBr were measured using a Balle–Flygare- (*25*) type pulsed-jet cavity Fourier transform microwave spectrometer (*26*). Two aluminum mirrors form the cavity; one is held fixed, while the other is used to tune the cavity to the microwave excitation frequency. Samples, entrained in a noble gas, are supersonically expanded in to the cavity from a nozzle situated slightly off center on the fixed mirror. Accordingly, all observed lines appear as Doppler doublets since the molecular jet and the axis of microwave propagation are parallel. The line frequencies are determined by taking the average of the Doppler components. In the present work the standard deviation of the frequency of a well-resolved line is estimated to be one-tenth the linewidth (ca. 1 kHz); for severely overlapped lines, this is increased to one-quarter the linewidth.

A description of the FTMW laser ablation system has been given elsewhere (*27*). AuCl and AuBr were generated by ablating gold foil (~98% purity, ~0.5-mm thick, wrapped

TABLE 1
Observed Transition Frequencies (in MHz) of $Au^{35}Cl$
in the $v = 0$, $v = 1$, and $v = 2$ Vibrational States

$J'-J''$	$F_1'-F_1''$	$F'-F''$	$v=0$	obs-calc	$v=1$	obs-calc	$v=2$	obs-calc
1-0	$\frac{3}{2}-\frac{3}{2}$	2-3	7008.5482	0.8[a]	6976.0420	0.2[a]	6943.5516	1.6[a]
	$\frac{3}{2}-\frac{3}{2}$	2-1	7008.5482	0.8	6976.0420	0.2	6943.5516	1.6
	$\frac{3}{2}-\frac{3}{2}$	2-2	7008.5482	-2.1	6976.0420	-2.4	6943.5516	-0.9
	$\frac{3}{2}-\frac{3}{2}$	1-1	7009.9585	1.9	6977.3572	3.3		
	$\frac{3}{2}-\frac{3}{2}$	1-2	7009.9585	-0.9	6977.3572	0.7		
	$\frac{3}{2}-\frac{3}{2}$	3-3	7010.0832	0.7	6977.4603	0.3	6944.8564	1.0
	$\frac{3}{2}-\frac{3}{2}$	3-2	7010.0832	-2.1	6977.4603	-2.4	6944.8564	-1.4
	$\frac{3}{2}-\frac{3}{2}$	0-1	7011.7053	-0.8				
	$\frac{5}{2}-\frac{3}{2}$	1-0	7024.0598	1.3	6991.5576	0.2		
	$\frac{5}{2}-\frac{3}{2}$	1-1	7024.0598	-1.6	6991.5576	-2.4		
	$\frac{5}{2}-\frac{3}{2}$	4-3	7024.7934	-0.4	6992.2468	-0.5	6959.7165	-0.2
	$\frac{5}{2}-\frac{3}{2}$	2-1	7025.3070	0.4	6992.7322	0.1	6960.1750	2.2
	$\frac{5}{2}-\frac{3}{2}$	2-2	7025.3070	-2.4	6992.7322	-2.5	6960.1750	-0.3
	$\frac{5}{2}-\frac{3}{2}$	3-3	7026.4185	2.5	6993.7427	2.8	6961.0857	0.6
	$\frac{5}{2}-\frac{3}{2}$	3-2	7026.4185	-0.5	6993.7427	0.1	6961.0857	-1.8
	$\frac{1}{2}-\frac{3}{2}$	1-1	7037.7534	0.9	7005.1784	2.8		
	$\frac{1}{2}-\frac{3}{2}$	1-2	7037.7534	-1.9	7005.1784	0.1		
	$\frac{1}{2}-\frac{3}{2}$	2-3	7037.9162	1.1	7005.3159	1.4	6972.7363	1.9
	$\frac{1}{2}-\frac{3}{2}$	2-2	7037.9162	-1.7	7005.3159	-1.2	6972.7363	-0.5
2-1	$\frac{3}{2}-\frac{1}{2}$	3-2	14028.5852	0.4	13963.4224	0.0	13898.2907	-0.9
	$\frac{3}{2}-\frac{1}{2}$	1-2	14028.5852	1.7	13963.4224	1.4		
	$\frac{3}{2}-\frac{1}{2}$	2-2	14028.5852	-2.0	13963.4224	-2.1	13898.2907	-2.9
	$\frac{3}{2}-\frac{1}{2}$	1-1	14028.7484	2.3	13963.5610	1.2	13898.4141	2.8
	$\frac{3}{2}-\frac{1}{2}$	2-1	14028.7484	-1.4	13693.5610	-2.4		
	$\frac{5}{2}-\frac{5}{2}$	1-2	14029.2700	-0.4				
	$\frac{5}{2}-\frac{5}{2}$	3-3	14029.4480	0.0	13964.3179	-0.1	13899.2174	-1.8
	$\frac{5}{2}-\frac{5}{2}$	2-2	14030.0090	-0.6	13964.8273	-0.6		
	$\frac{5}{2}-\frac{5}{2}$	4-4	14030.3274	0.4	13965.1221	1.1	13899.9510	0.8
	$\frac{5}{2}-\frac{5}{2}$	1-1	14030.5170	1.3				
	$\frac{5}{2}-\frac{5}{2}$	3-2	14030.5570	-0.6				
	$\frac{3}{2}-\frac{5}{2}$	3-2	14041.1936	0.4				
	$\frac{3}{2}-\frac{5}{2}$	3-4	14041.7074	1.4				
	$\frac{5}{2}-\frac{3}{2}$	1-0	14042.8709	0.0	13977.9198	0.9		
	$\frac{1}{2}-\frac{1}{2}$	2-2	14044.1325	0.4	13978.9823	0.2	13913.8645	0.3
	$\frac{1}{2}-\frac{1}{2}$	1-2	14044.2230	-0.9	13979.0621	1.5		
	$\frac{7}{2}-\frac{5}{2}$	2-2					13914.1260	0.3
	$\frac{1}{2}-\frac{1}{2}$	2-1	14044.2951	0.4	13979.1204	-0.6		
	$\frac{1}{2}-\frac{1}{2}$	1-1	14044.3852	-1.3				

[a] Residuals in kHz.

around a 4-mm-diameter glass rod), using the second harmonic (532 nm) of a Nd:YAG laser, in the presence of 0.1% Cl_2 or Br_2 in ultrahigh-purity Ar or Ne carrier gas, at backing pres-sures of 5–7 atm. The choice of carrier gas depended on the transitions sought: argon was used for molecules in the ground vibrational state, and neon was used for those in excited

TABLE 1—*Continued*

$J'-J''$	$F_1'-F_1''$	$F'-F''$	$v=0$	obs-calc	$v=1$	obs-calc	$v=2$	obs-calc
	$\frac{5}{2}-\frac{3}{2}$	1-1	14044.6206	0.1[a]	13979.5183	-0.6[a]		
	$\frac{5}{2}-\frac{3}{2}$	4-3	14045.0385	0.1	13979.9088	0.6	14914.8108	-0.7[a]
	$\frac{7}{2}-\frac{5}{2}$	5-4	14045.4340	0.1	13980.2760	0.1	13915.1520	-0.1
	$\frac{7}{2}-\frac{5}{2}$	2-1	14045.5175	-0.5				
	$\frac{7}{2}-\frac{5}{2}$	4-3	14045.8269	-0.3	13980.6410	-0.4	13915.4899	-0.5
	$\frac{7}{2}-\frac{5}{2}$	3-2	14046.1927	0.0	13980.9583	-0.4	13915.7643	0.1
	$\frac{5}{2}-\frac{3}{2}$	2-2	14046.7692	0.4				
	$\frac{5}{2}-\frac{3}{2}$	3-2	14047.3170	0.2	13982.0160	-0.2	13916.7542	-0.1
	$\frac{7}{2}-\frac{5}{2}$	4-4	14047.4501	0.5	13982.1346	0.5	13916.8601	1.4
	$\frac{3}{2}-\frac{3}{2}$	1-0	14054.7925	0.0				
	$\frac{3}{2}-\frac{3}{2}$	3-3	14056.4179	0.5	13991.2775	0.7	13926.1711	0.5
	$\frac{3}{2}-\frac{3}{2}$	2-3	14056.4179	-1.9				
	$\frac{3}{2}-\frac{3}{2}$	2-1	14056.5464	0.7	13991.3849	-0.2	13926.2608	-0.6
	$\frac{3}{2}-\frac{3}{2}$	1-2	14057.9530	1.8				
	$\frac{3}{2}-\frac{3}{2}$	3-2	14057.9530	0.6	13992.6933	-1.8	13927.4752	-0.8
	$\frac{3}{2}-\frac{3}{2}$	2-2	14057.9530	-1.9	13992.6933	-3.9	13927.4752	-2.7
	$\frac{1}{2}-\frac{3}{2}$	2-3	14071.9647	0.0				
	$\frac{1}{2}-\frac{3}{2}$	1-1	14072.1828	0.4				
3-2	$\frac{7}{2}-\frac{7}{2}$	4-4	21051.1607	-0.3				
	$\frac{7}{2}-\frac{7}{2}$	3-3	21051.3152	-0.5				
	$\frac{7}{2}-\frac{7}{2}$	5-5	21051.7456	0.6	20953.9545	0.8		
	$\frac{3}{2}-\frac{1}{2}$	0-1	21061.2064	0.0				
	$\frac{5}{2}-\frac{3}{2}$	1-1	21062.1390	1.5	20964.4642	2.1		
	$\frac{5}{2}-\frac{3}{2}$	1-0	21062.1390	-0.6				
	$\frac{3}{2}-\frac{1}{2}$	1-1	21062.8323	1.2				
	$\frac{3}{2}-\frac{1}{2}$	3-2	21062.8965	-0.2	20965.1591	0.3	20867.4712	-0.3
	$\frac{5}{2}-\frac{3}{2}$	4-3	21063.0137	-0.3	20965.2567	-0.2	20867.5515	-1.4
	$\frac{5}{2}-\frac{3}{2}$	2-1	21063.5476	-0.6	20965.7549	2.3	20868.0103	-0.4
	$\frac{5}{2}-\frac{3}{2}$	3-2	21064.0923	-0.5	20966.2633	-1.0	20868.4890	-0.3
	$\frac{3}{2}-\frac{1}{2}$	2-1	21064.3277	-0.5	20966.4882	-0.6		
	$\frac{3}{2}-\frac{1}{2}$	2-2	21064.4195	-0.6	20966.5669	-0.3		
	$\frac{9}{2}-\frac{7}{2}$	3-3	21065.1365	0.3				
	$\frac{7}{2}-\frac{5}{2}$	2-2	21065.9226	0.3				
	$\frac{7}{2}-\frac{5}{2}$	5-4	21066.8524	0.5	20969.1081	-0.6	20871.4171	0.5
	$\frac{9}{2}-\frac{7}{2}$	6-5	21067.0097	0.0	20969.2557	0.0	20871.5534	0.4
	$\frac{9}{2}-\frac{7}{2}$	3-2	21067.0565	0.3				
	$\frac{9}{2}-\frac{7}{2}$	5-4	21067.1661	0.0	20969.4008	-0.6	20871.6889	0.7

vibrational states. This procedure followed recent experience with the copper(I) and silver(I) monohalides, Cu*X* and Ag*X* (*X* = F, Cl, Br), for which lines from excited vibrational states could not be observed with argon as the backing gas. This was also found to be the case for AuCl and AuBr (though not for some other molecules studied earlier in this laboratory, such as ZrO (*28*), ScCl (*21*), or YBr (*20*)).

THEORETICAL CALCULATIONS

The geometries of AuF, AuCl, and AuBr were optimized at the second-order Møller–Plesset (MP2) (*29*) level of theory using the GAUSSIAN 98 suite of programs (*30*). For Au, a relativistic effective core potential (RECP) was used (*5*). The basis set used for gold was a (9*s*/7*p*/6*d*/3*f*) Gaussian basis set

TABLE 1—*Continued*

$J'-J''$	$F_1'-F_1''$	$F'-F''$	$v=0$	obs-calc	$v=1$	obs-calc	$v=2$	obs-calc
	$\frac{9}{2}-\frac{7}{2}$	4-3	21067.2245	-0.6[a]	20969.4578	-2.2[a]	20871.7465	0.7[a]
	$\frac{7}{2}-\frac{5}{2}$	3-2	21067.4984	-0.4	20969.7007	0.3	20871.9574	1.4
	$\frac{7}{2}-\frac{5}{2}$	4-3	21067.5406	0.4	20969.7509	1.3	20872.0099	-0.8
	$\frac{9}{2}-\frac{7}{2}$	5-5	21069.1822	0.5				
	$\frac{5}{2}-\frac{5}{2}$	4-4	21074.3932	0.2	20976.6255	0.0	20878.9128	0.8
	$\frac{5}{2}-\frac{5}{2}$	2-2	21074.7302	-0.4				
	$\frac{5}{2}-\frac{5}{2}$	3-3	21074.7302	-0.7				
	$\frac{3}{2}-\frac{3}{2}$	3-3	21078.4436	-0.4	20980.7181	-0.4		

contracted to $(8s/4p/5d/3f)$ (*5, 31*). For F we used the aug-cc-pVTZ basis set (*32*), while for Cl and Br we used the aug-cc-pVDZ basis set (*33*).

RESULTS

The search for the pure rotational lines from the ground vibrational state of $Au^{35}Cl$ was initiated using the molecular parameters obtained in Ref. (*24*). Lines from the $J = 2-1$ transition of $Au^{35}Cl$ were found within 2 MHz of the predicted frequency. Further confirmation that the lines emanated from AuCl was made by the prediction and measurement of lines from $Au^{37}Cl$. The strongest lines for $Au^{35}Cl$ were easily seen in 10 pulses. A portion of the hyperfine structure of the $J = 2-1$ transition of $Au^{35}Cl$ is shown in Fig. 1. These results, combined with those given in Ref. (*24*), were then used to predict line frequencies of both isotopomers in their excited vibrational states; these were equally easily found.

Altogether, lines from the $J = 1-0$ to $J = 3-2$ transitions were measured and assigned to the $v = 0$, 1, and 2 vibrational states of $Au^{35}Cl$ and the $v = 0$ and $v = 1$ vibrational states of $Au^{37}Cl$. In assigning and fitting the measured frequencies, the coupling scheme $\mathbf{F}_1 = \mathbf{J} + \mathbf{I}_{Cl}$, $\mathbf{F} = \mathbf{F}_1 + \mathbf{I}_{Au}$ was employed, where ^{197}Au (100% abundance), ^{35}Cl (74.5%), and ^{37}Cl (25.5%) each have a nuclear spin of $I = 3/2$. The measured frequencies with their assignments are listed in Tables 1 and 2.

The observed spectra have been interpreted in terms of the Hamiltonian,

$$\mathbf{H} = \mathbf{H}_{rot} + \mathbf{H}_{elec\ quad} + \mathbf{H}_{spin-rot}, \quad [1]$$

where

$$\mathbf{H}_{rot} = B_v\mathbf{J}^2 - D_J\mathbf{J}^4 \quad [2]$$

$$\mathbf{H}_{elec\ quad} = -\frac{1}{6}(\mathbf{V}_{Au}^{(2)}\mathbf{Q}_{Au}^{(2)} + \mathbf{V}_X^{(2)}\mathbf{Q}_X^{(2)}) \quad [3]$$

$$\mathbf{H}_{spin-rot} = C_I(Au)\mathbf{I}_{(Au)} \cdot \mathbf{J} + C_I(X)\mathbf{I}_X \cdot \mathbf{J}. \quad [4]$$

In Eqs. [3] and [4], X refers to the halogen. Line frequencies were fitted within experimental uncertainty using Pickett's weighted least-squares program SPFIT (*34*). The resulting molecular constants for $Au^{35}Cl$ and $Au^{37}Cl$ are listed in Table 3.

Since there have been no previous spectroscopic studies on AuBr, its bond length was taken from the theoretical study on Au(I) diatomics by Schwerdtfeger *et al.* (*5*). This was further refined using the ratio of the observed r_e of AuCl to its predicted value given in Ref. (*5*) [at the CEPA-1 level of theory]. Lines from the $J = 3-2$ transition of the ground vibrational state of $Au^{79}Br$ were found within 10 MHz of the predicted frequency. Similar accuracy was found for AuF after scaling the *ab initio* calculated bond length (*22*). Confirmation that the lines were from AuBr was made by the prediction and measurement of lines from $Au^{81}Br$ as well as from the ratio of the nuclear quadrupole coupling constants of ^{79}Br and ^{81}Br, which agreed with the ratio of their quadrupole moments. A portion of the hyperfine structure from the $J = 4-3$ transition
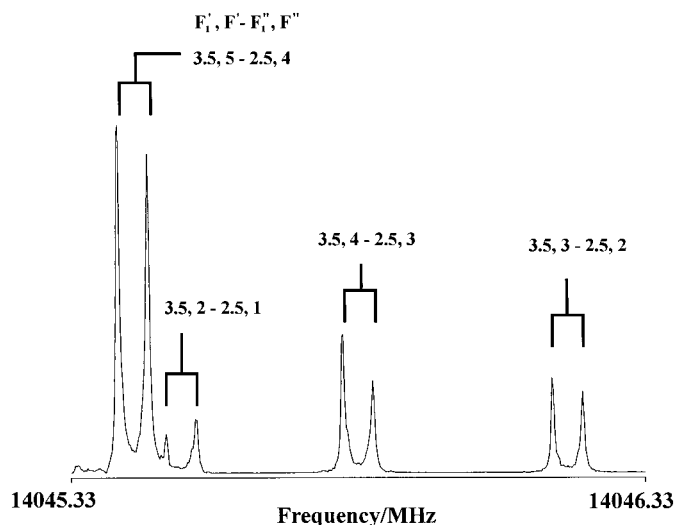

FIG. 1. A portion of the hyperfine structure of the $J = 2-1$ transition of $Au^{35}Cl$ in the ground vibrational state. Experimental conditions: 0.1% Cl_2 in argon; backing pressure, 5–7 bar; microwave pulse width, 0.8 μs; number of scans, 100; 4K transform.

TABLE 2
Observed Transition Frequencies (in MHz) of Au^{37}Cl in the $v = 0$ and $v = 1$ Vibrational States[a]

$J'-J''$	$F'_1-F''_1$	$F'-F''$	$v=0$	obs-calc	$v=1$	obs-calc	$J'-J''$	$F'_1-F''_1$	$F'-F''$	$v=0$	obs-calc	$v=1$	obs-calc
1-0	$\frac{3}{2}-\frac{3}{2}$	2-3	6689.3465	1.2[a]	6659.0626	2.1[a]		$\frac{7}{2}-\frac{5}{2}$	3-2	13402.3673	0.0	13341.5556	-1.2
	$\frac{3}{2}-\frac{3}{2}$	2-1	6689.3465	1.2	6659.0626	2.1		$\frac{5}{2}-\frac{5}{2}$	2-2	13402.8401	-0.2	13342.0288	0.0
	$\frac{3}{2}-\frac{3}{2}$	2-2	6689.3465	-1.2	6659.0626	-0.1		$\frac{5}{2}-\frac{5}{2}$	3-2	13403.4204	0.1	13342.5550	0.0
	$\frac{3}{2}-\frac{3}{2}$	3-3	6690.8808	1.0	6660.4806	-0.5		$\frac{7}{2}-\frac{5}{2}$	4-4	13403.5710	0.4	13342.6878	-0.5
	$\frac{3}{2}-\frac{3}{2}$	3-2	6690.8808	-1.4	6660.4806	-2.7		$\frac{3}{2}-\frac{3}{2}$	3-3	13410.1952	0.0	13349.4797	0.9
	$\frac{3}{2}-\frac{3}{2}$	1-1	6690.7156	1.5				$\frac{3}{2}-\frac{3}{2}$	2-3	13410.1952	-2.1	13349.4797	-1.0
	$\frac{3}{2}-\frac{3}{2}$	1-2	6690.7156	-0.8				$\frac{3}{2}-\frac{3}{2}$	0-1	13410.3635	5.0		
	$\frac{3}{2}-\frac{3}{2}$	0-1	6692.5254	-0.3				$\frac{3}{2}-\frac{3}{2}$	2-1	13410.3635	0.4	13349.6196	-1.1
	$\frac{5}{2}-\frac{3}{2}$	1-0	6701.6344	0.6				$\frac{3}{2}-\frac{3}{2}$	1-2	13411.7297	0.9		
	$\frac{5}{2}-\frac{3}{2}$	1-1	6701.6344	-1.7				$\frac{3}{2}-\frac{3}{2}$	3-2	13411.7297	-0.1	13350.9026	3.2
	$\frac{5}{2}-\frac{3}{2}$	4-3	6702.3276	-0.5	6671.9953	-0.2		$\frac{3}{2}-\frac{3}{2}$	2-2	13411.7297	-2.1	13350.9026	1.3
	$\frac{5}{2}-\frac{3}{2}$	2-1	6702.8002	0.6	6672.4460	0.5		$\frac{1}{2}-\frac{3}{2}$	2-3	13422.4789	0.2		
	$\frac{5}{2}-\frac{3}{2}$	2-2	6702.8002	-1.7	6672.4460	-1.6		$\frac{1}{2}-\frac{3}{2}$	1-1	13422.7578	-1.3		
	$\frac{5}{2}-\frac{3}{2}$	3-2	6703.9751	-0.1	6673.5136	0.7	3-2	$\frac{7}{2}-\frac{7}{2}$	4-4	20088.8252	0.2		
	$\frac{5}{2}-\frac{3}{2}$	3-3	6703.9751	2.3	6673.5136	2.9		$\frac{7}{2}-\frac{7}{2}$	3-3	20088.9784	-0.4		
	$\frac{1}{2}-\frac{3}{2}$	1-1	6712.6790	1.6	6682.3086	0.4		$\frac{7}{2}-\frac{7}{2}$	5-5	20089.4557	-0.3		
	$\frac{1}{2}-\frac{3}{2}$	1-2	6712.6790	-0.8	6682.3086	-1.8		$\frac{3}{2}-\frac{1}{2}$	0-1	20096.4137	0.4		
	$\frac{1}{2}-\frac{3}{2}$	2-3	6712.8823	0.6	6682.4857	2.0		$\frac{5}{2}-\frac{3}{2}$	1-1	20097.3668	1.0		
	$\frac{1}{2}-\frac{3}{2}$	2-2	6712.8823	-1.7	6682.4857	-0.2		$\frac{5}{2}-\frac{3}{2}$	1-0	20097.3668	-0.5		
2-1	$\frac{3}{2}-\frac{1}{2}$	3-2	13388.1934	0.0	13327.4772	1.0		$\frac{3}{2}-\frac{1}{2}$	3-2	20098.1447	1.5	20007.0538	0.1
	$\frac{3}{2}-\frac{1}{2}$	1-2	13388.1934	1.0				$\frac{5}{2}-\frac{3}{2}$	4-3	20098.3007	0.2	20007.1863	0.1
	$\frac{3}{2}-\frac{1}{2}$	2-2	13388.1934	-2.0				$\frac{5}{2}-\frac{3}{2}$	2-1	20098.8214	-1.0	20007.6711	-2.8
	$\frac{3}{2}-\frac{1}{2}$	0-1	13388.3971	2.0				$\frac{5}{2}-\frac{3}{2}$	3-2	20099.3363	0.1	20008.1600	0.3
	$\frac{3}{2}-\frac{1}{2}$	1-1	13388.3971	0.5	13327.6511	0.4		$\frac{3}{2}-\frac{1}{2}$	2-1	20099.5457	-0.4		
	$\frac{3}{2}-\frac{1}{2}$	2-1	13388.3971	-2.6	13327.6511	-2.5		$\frac{3}{2}-\frac{1}{2}$	2-2	20099.6600	-0.7		
	$\frac{5}{2}-\frac{5}{2}$	3-3	13388.7903	-2.5	13328.1056	0.7		$\frac{7}{2}-\frac{5}{2}$	2-1			20010.0218	3.0
	$\frac{5}{2}-\frac{5}{2}$	2-2	13389.3865	0.5				$\frac{7}{2}-\frac{5}{2}$	2-2	20100.3802	0.4		
	$\frac{5}{2}-\frac{5}{2}$	4-4	13389.7062	0.1	13328.9400	1.0		$\frac{7}{2}-\frac{5}{2}$	5-4	20101.2906	-0.1	20010.1948	0.5
	$\frac{3}{2}-\frac{5}{2}$	3-4	13398.7477	0.7				$\frac{9}{2}-\frac{7}{2}$	6-5	20101.4435	-0.3	20010.3377	0.2
	$\frac{5}{2}-\frac{3}{2}$	1-0	13398.9379	0.1				$\frac{9}{2}-\frac{7}{2}$	3-2	20101.4748	2.6		
	$\frac{3}{2}-\frac{5}{2}$	2-1	13399.4422	1.2				$\frac{9}{2}-\frac{7}{2}$	5-4	20101.5958	-0.2	20010.4799	0.2
	$\frac{1}{2}-\frac{1}{2}$	2-2	13400.4774	0.5	13339.7637	-0.6		$\frac{9}{2}-\frac{7}{2}$	4-3	20101.6388	-0.9	20010.5245	-0.8
	$\frac{1}{2}-\frac{1}{2}$	1-2	13400.5914	-0.1	13339.8633	0.3		$\frac{7}{2}-\frac{5}{2}$	4-3	20101.9586	0.5	20010.8221	2.8
	$\frac{1}{2}-\frac{1}{2}$	2-1	13400.6811	-0.1	13339.9402	0.4		$\frac{7}{2}-\frac{5}{2}$	3-2	20101.9586	-1.4	20010.8065	0.0
	$\frac{5}{2}-\frac{3}{2}$	1-1	13400.7497	0.3	13340.0730	-0.9		$\frac{9}{2}-\frac{7}{2}$	5-5	20103.6256	-0.2		
	$\frac{5}{2}-\frac{3}{2}$	4-3	13401.1543	0.0	13340.4546	1.2		$\frac{5}{2}-\frac{5}{2}$	1-1	20106.9756	-0.8		
	$\frac{7}{2}-\frac{5}{2}$	5-4	13401.5406	-0.2	13340.8127	-1.2		$\frac{5}{2}-\frac{5}{2}$	4-4	20107.3415	0.1		
	$\frac{7}{2}-\frac{5}{2}$	2-1	13401.6241	-0.2				$\frac{3}{2}-\frac{3}{2}$	3-3	20110.4265	-0.3		
	$\frac{7}{2}-\frac{5}{2}$	4-3	13401.9254	-0.4[a]	13341.1722	-0.9[a]							

[a] Residuals in kHz.

of Au^{81}Br is shown in Fig. 2. The vibration–rotation constant, α_e, for AuBr was predicted by using the relationship between the α_e of AgCl (35), AuCl, and AgBr (36). Lines from vibrationally excited AuBr were found to be considerably weaker than those of AuCl, so that lines from only the first excited vibrational state were observed. In all, lines from the $J = 2–1$ to $J = 5–4$ transitions were measured and assigned to the $v = 0$ and $v = 1$ vibrational states of Au^{79}Br and Au^{81}Br. The measured frequencies and their assignments are listed in Table 4. In assigning the measured lines, the coupling scheme $\mathbf{F}_1 =$ $\mathbf{J} + \mathbf{I}_{Br}$, $\mathbf{F} = \mathbf{F}_1 + \mathbf{I}_{Au}$ was employed, where ^{79}Br (50.5%) and ^{81}Br (49.5%) also have a nuclear spin of $I = 3/2$. The spectral analyses followed the same procedure as for AuCl; the resulting constants are listed in Table 5.

DISCUSSION

Tables 3 and 5 contain a large number of accurate spectroscopic constants for both AuCl and AuBr. From the values obtained earlier (B_v and D_{Jv} of Au^{35}Cl), the present results are

TABLE 3
Molecular Constants Calculated for $Au^{35}Cl$ and $Au^{37}Cl$ in MHz[a]

$Au^{35}Cl$				
Parameters	$v=0$	$v=1$	$v=2$	Lit. Value[b]
B_v	3511.087771(85)	3494.793905(97)	3478.50879(11)	3511.06(19)
$D_{Jv} \times 10^3$	1.3182(53)	1.3233(65)	1.3363(74)	1.325(22)
$eQq(Au)_v$	9.63312(13)	8.8969(18)	8.1861(25)	
$eQq(Cl)_v$	−61.99694(81)	−62.0831(12)	−62.1663(15)	
$C_I(Au) \times 10^4$	3.34(85)	3.6(11)	3.34[c]	
$C_I(Cl) \times 10^4$	2.61(76)	2.61[c]	2.61[c]	
$Au^{37}Cl$				
Parameters	$v=0$	$v=1$		
B_v	3350.184209(89)	3334.99834(11)		
$D_{Jv} \times 10^3$	1.2016(56)	1.2053(74)		
$eQq(Au)_v$	9.6415(14)	8.9222(25)		
$eQq(Cl)_v$	−48.85934(88)	−48.9227(14)		
$C_I(Au) \times 10^4$	2.66(93)	2.66[c]		
$C_I(Cl) \times 10^4$	1.95(78)	1.95[c]		

[a] Numbers in parentheses are one standard deviation in units of last significant figure.

[b] Results from electronic study Ref. (24), for $v=0$.

[c] Fixed to ground state value.

within the uncertainties previously quoted (24) and are considerably more precise. All other constants, namely rotational constants B_v, centrifugal distortion constants D_{Jv}, nuclear quadrupole coupling constants eQq for all atoms, and nuclear spin–rotation constants C_I are newly evaluated. They have been used to obtain further information about the molecules.

The equilibrium rotational constant B_e and the vibration–rotation constants α_e and γ_e for AuCl and AuBr were calculated using the expression:

$$B_v = B_e - \alpha_e(v + 1/2) + \gamma_e(v + 1/2)^2. \qquad [5]$$
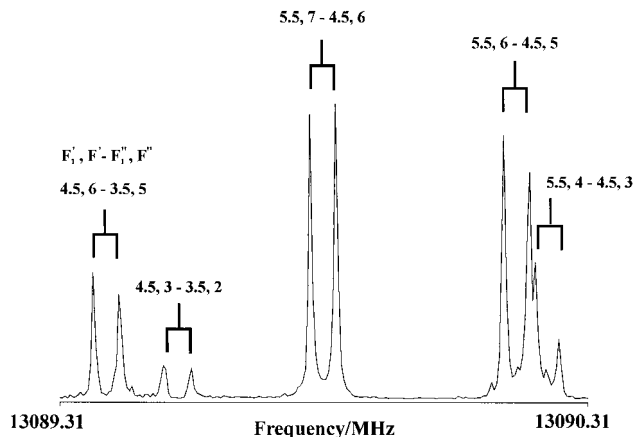

FIG. 2. A portion of the hyperfine structure of the $J = 4-3$ transition of $Au^{81}Br$ in the ground vibrational state. Experimental conditions: 0.1% Br_2 in argon; backing pressure, 5–7 bar; microwave pulse width, 0.8 μs; number of scans, 100; 4K transform.

The results are listed in Tables 6 and 7 for AuCl and AuBr, respectively. Since lines from three vibrational states were measured for $Au^{35}Cl$, all three vibration–rotation constants in Eq. [5] could be determined. The resulting values of B_e and α_e of $Au^{35}Cl$ are in good agreement with those from the electronic study (24). For $Au^{37}Cl$, for which there are data for only two vibrational states, B_e and α_e were determined by fixing γ_e to the $Au^{35}Cl$ value. For AuBr, the values in Table 7 were obtained assuming $\gamma_e = 0$.

The equilibrium bond lengths, r_e, obtained from the B_e values, are also listed in Tables 6 and 7. The uncertainties given reflect those of the rotational constants, fundamental constants, and atomic masses. For AuCl, the r_e values are two orders of magnitude more precise than the one from the electronic spectrum (24). For AuBr, if γ_e is estimated as being in the same ratio to α_e as in AuCl, the r_e could be lower by $\sim 7 \times 10^{-7}$ Å. For both molecules, the isotopic variation in r_e is less than the uncertainties, indicating that the Born–Oppenheimer approximation holds well.

The harmonic vibration frequency, ω_e, and the vibrational anharmonicity constant, $\omega_e x_e$, of AuCl and AuBr were estimated using the relations developed by Kratzer (37) and Pekeris (38), respectively. They assume a Morse potential,

$$\omega_e = \sqrt{\frac{4B_e^3}{D_{Je}}} \qquad [6]$$

$$\omega_e x_e = B_e \left(\frac{\alpha_e \omega_e}{6B_e^2} + 1 \right)^2, \qquad [7]$$

TABLE 4
Observed Transition Frequencies (in MHz) of $Au^{79}Br$ and $Au^{81}Br$ in the $v = 0$ and $v = 1$ Vibrational States

| | Assignment | | | $Au^{79}Br$ | | | | $Au^{81}Br$ | | |
$J'-J''$	$F_1'-F_1''$	$F'-F''$	$v=0$	obs-calc	$v=1$	obs-calc	$v=0$	obs-calc	$v=1$	obs-calc
2-1	$\frac{3}{2}-\frac{3}{2}$	3-3	6565.7367	-0.6[a]			6463.9892	0.0[a]		
	$\frac{3}{2}-\frac{3}{2}$	2-2	6571.5014	0.6			6469.7901	0.0		
	$\frac{3}{2}-\frac{3}{2}$	1-2	6571.6733	3.8			6469.9315	0.9		
	$\frac{3}{2}-\frac{3}{2}$	3-2	6571.6733	1.1			6469.9315	-1.6		
	$\frac{5}{2}-\frac{3}{2}$	1-0	6643.6777	0.9			6528.0856	1.2		
	$\frac{7}{2}-\frac{5}{2}$	2-2	6646.7023	0.8			6530.8808	1.0		
	$\frac{5}{2}-\frac{3}{2}$	4-3	6650.9485	-1.5	6628.8619	0.6[a]	6535.2914	-1.5	6513.7892	0.4[a]
	$\frac{7}{2}-\frac{5}{2}$	3-3	6651.4933	2.1			6535.7736	1.2		
	$\frac{5}{2}-\frac{3}{2}$	2-1	6652.3459	0.8			6536.6978	1.1		
	$\frac{7}{2}-\frac{5}{2}$	5-4	6652.9153	-1.3	6630.8011	0.3	6537.1919	-1.0	6515.6611	-0.2
	$\frac{7}{2}-\frac{5}{2}$	2-1	6653.2205	0.3			6537.4874	0.5		
	$\frac{7}{2}-\frac{5}{2}$	3-2	6654.3981	-0.3	6632.2642	-1.9	6538.5856	-0.2	6517.0401	-0.7
	$\frac{7}{2}-\frac{5}{2}$	4-3	6654.5830	-0.7	6632.4394	-0.2	6538.8739	-0.8	6517.3151	0.4
	$\frac{5}{2}-\frac{3}{2}$	2-2	6658.4626	0.2			6542.8559	0.8		
	$\frac{5}{2}-\frac{3}{2}$	3-2	6660.0189	0.3			6544.3804	0.6		
	$\frac{7}{2}-\frac{5}{2}$	4-4					6544.6829	1.7		
	$\frac{1}{2}-\frac{1}{2}$	2-1	6664.0142	-0.8			6546.6428	-0.5		
	$\frac{1}{2}-\frac{1}{2}$	1-2	6664.1485	-1.3			6546.7977	-1.6		
	$\frac{1}{2}-\frac{1}{2}$	2-2	6664.3323	1.4			6547.0206	1.2		
	$\frac{5}{2}-\frac{5}{2}$	3-3	6775.3763	-0.7			6639.3849	-0.4		
	$\frac{5}{2}-\frac{5}{2}$	4-4	6778.0903	1.0			6642.0501	1.2		
	$\frac{3}{2}-\frac{1}{2}$	2-1					6650.5352	-2.7		
	$\frac{3}{2}-\frac{1}{2}$	1-1	6788.7351	-2.4			6650.6762	-2.3		
	$\frac{3}{2}-\frac{1}{2}$	2-2	6788.8850	0.3						
	$\frac{3}{2}-\frac{1}{2}$	3-2	6789.0569	0.8			6651.0584	1.3		
3-2	$\frac{3}{2}-\frac{3}{2}$	3-3	9894.7025	0.5			9735.1744	0.0		
	$\frac{3}{2}-\frac{3}{2}$	1-2	9894.7965	-1.8						
	$\frac{5}{2}-\frac{5}{2}$	4-4	9933.0681	0.1			9767.0219	0.9		
	$\frac{5}{2}-\frac{5}{2}$	2-2	9933.3877	-0.2			9767.2686	-0.2		
	$\frac{5}{2}-\frac{5}{2}$	3-3	9934.7529	0.1			9768.7337	0.4		
	$\frac{9}{2}-\frac{7}{2}$	3-3	9982.6766	1.4						
	$\frac{7}{2}-\frac{5}{2}$	2-2	9985.3340	0.3						
	$\frac{9}{2}-\frac{7}{2}$	4-4	9987.9562	1.4						
	$\frac{7}{2}-\frac{5}{2}$	2-1	9988.4252	1.3			9813.3276	0.3		
	$\frac{7}{2}-\frac{5}{2}$	5-4	9988.9720	-1.4	9955.8081	-0.9	9813.8497	-1.0	9781.5604	-0.8

[a] Residuals in kHz.

where D_{Je} is the equilibrium centrifugal distortion constant, which is approximated as the ground state value, D_{J0}. The dissociation energy D_e can be approximated by the relation (39)

$$D_e \sim \frac{\omega_e^2}{4\omega_e x_e}. \quad [8]$$

These expressions have been found to provide reasonable estimates of ω_e, $\omega_e x_e$, and D_e for ScF and ScCl (21). The results for AuCl and AuBr are listed in Tables 6 and 7, respectively. For AuCl, the harmonic frequency (ω_e) is in good agreement with the result from the electronic study (24). The new value for the anharmonicity constant, $\omega_e x_e$, differs considerably from the value in Ref. (23); however, since the latter

TABLE 4—*Continued*

Assignment			Au^{79}Br				Au^{81}Br			
$J'-J''$	$F_1'-F_1''$	$F'-F''$	$v=0$	obs-calc	$v=1$	obs-calc	$v=0$	obs-calc	$v=1$	obs-calc
	$\frac{7}{2}-\frac{5}{2}$	3-3					9814.3982	0.6[a]		
	$\frac{9}{2}-\frac{7}{2}$	6-5	9989.7953	-1.1[a]	9956.6202	-0.3[a]	9814.6492	-0.7	9782.3485	0.0[a]
	$\frac{9}{2}-\frac{7}{2}$	3-2	9990.3721	0.0	9957.1847	0.0	9815.2496	0.5	9782.9371	1.5
	$\frac{9}{2}-\frac{7}{2}$	5-4	9990.4983	-0.8	9957.3114	0.5	9815.3607	-0.8	9783.0470	-0.7
	$\frac{9}{2}-\frac{7}{2}$	4-3	9991.0465	-0.8	9957.8489	0.3	9815.9297	0.6	9783.6037	-0.6
	$\frac{7}{2}-\frac{5}{2}$	3-2	9991.0669	1.0	9957.8706	1.4	9815.9216	-0.7	9783.6037	2.2
	$\frac{7}{2}-\frac{5}{2}$	4-3	9991.8861	-0.2	9958.6732	-0.4	9816.7722	-0.1	9784.4343	-0.6
	$\frac{7}{2}-\frac{5}{2}$	4-4	9995.0201	0.0			9819.9156	0.4		
	$\frac{9}{2}-\frac{7}{2}$	5-5	9998.0140	1.8						
	$\frac{3}{2}-\frac{1}{2}$	0-1	10013.7746	-0.4						
	$\frac{5}{2}-\frac{3}{2}$	1-0	10015.7897	0.3			9835.9180	0.7		
	$\frac{5}{2}-\frac{3}{2}$	1-1	10016.0068	-0.1			9836.1082	0.0		
	$\frac{5}{2}-\frac{3}{2}$	4-3	10018.2798	-0.9	9985.1572	0.0	9838.3242	-0.5	9806.0705	0.0
	$\frac{3}{2}-\frac{1}{2}$	3-2	10019.4275	0.2			9839.2113	-0.8		
	$\frac{3}{2}-\frac{1}{2}$	1-1	10019.5324	-0.8			9839.3396	-0.9		
	$\frac{5}{2}-\frac{3}{2}$	2-1	10020.1813	0.5			9840.1936	0.4		
	$\frac{5}{2}-\frac{3}{2}$	2-2	10020.3488	-0.7			9840.3345	0.7		
	$\frac{5}{2}-\frac{3}{2}$	3-3	10023.0984	-0.8						
	$\frac{5}{2}-\frac{3}{2}$	3-2	10023.2708	0.2			9843.3232	0.2		
	$\frac{3}{2}-\frac{1}{2}$	2-2	10025.3574	-1.9			9845.1493	-1.5		
	$\frac{3}{2}-\frac{1}{2}$	2-1	10025.5416	1.2			9845.3721	1.2		
	$\frac{7}{2}-\frac{7}{2}$	5-5	10114.1474	1.3			9918.7085	1.9		
4-3	$\frac{5}{2}-\frac{5}{2}$	4-4	13213.9924	0.6			12997.9359	0.0		
	$\frac{7}{2}-\frac{7}{2}$	2-2	13281.1224	-1.3						
	$\frac{7}{2}-\frac{7}{2}$	5-5	13281.4156	0.9			13054.0804	1.0		
	$\frac{7}{2}-\frac{7}{2}$	3-3	13281.5198	-0.7			13054.1140	-2.6		
	$\frac{7}{2}-\frac{7}{2}$	4-4	13282.1281	0.1			13054.8068	-0.6		
	$\frac{9}{2}-\frac{7}{2}$	6-5	13323.5588	-0.5	13279.3293	-0.3	13089.4009	-0.7	13046.3376	0.2
	$\frac{9}{2}-\frac{7}{2}$	3-2	13323.6838	0.8	13279.4515	0.7	13089.5344	1.0	13046.4663	0.2
	$\frac{11}{2}-\frac{9}{2}$	7-6	13323.9788	-0.9	13279.7433	-0.8	13089.8102	-0.6	13046.7387	-1.8
	$\frac{11}{2}-\frac{9}{2}$	6-5	13324.3391	-0.3	13280.0987	1.2	13090.1745	-1.2	13047.0994	0.4
	$\frac{11}{2}-\frac{9}{2}$	4-3	13324.3907	-1.5	13280.1481	-1.1	13090.2324	1.0	13047.1535	0.0
	$\frac{11}{2}-\frac{9}{2}$	5-4	13324.7076	-0.0	13280.4607	0.9	13090.5432	-0.1	13047.4616	0.9
	$\frac{9}{2}-\frac{7}{2}$	5-4	13324.8275	-0.6	13280.5772	-0.6	13090.6693	-0.9	13047.5862	0.5
	$\frac{9}{2}-\frac{7}{2}$	4-3	13324.8938	1.3	13280.6434	1.4	13090.7260	0.7	13047.6398	-1.0
	$\frac{7}{2}-\frac{5}{2}$	2-2					13096.7361	-2.5		

came from a 1928 study of the electronic spectrum, where the resolution was ~0.5 cm^{-1}, the discrepancy is not unreasonable. For AuBr, the present values are the first obtained experimentally.

For AuCl and AuBr, there are several published quantum chemical predictions of their properties, including those in Refs. (*5, 7, 9, 10, 12*). For AuCl, the most accurate predicted value of r_e is from MP2 results in Ref. (*9*). Our own MP2 results using a slightly different basis set, as given above,

improve the agreement a little; this is shown in Table 8. For ω_e, the same calculations produce a very reasonable value, but the CEPA-1 value in Ref. (*5*) shows better agreement with our estimates. The Douglas–Kroll DFT value of the dissociation energy D_e in Ref. (*11*) is very close to our estimate. For AuBr, whose theoretical literature is less extensive, the CEPA-1 calculation in Ref. (*5*) provides moderately good values of r_e and ω_e. The calculated r_e and ω_e values in the present work (Table 8) show much better agreement with experiment.

TABLE 4—*Continued*

	Assignment		Au^{79}Br				Au^{81}Br			
J'-J''	F'_1-F''_1	F'-F''	$v=0$	obs-calc	$v=1$	obs-calc	$v=0$	obs-calc	$v=1$	obs-calc
	$\frac{9}{2}$-$\frac{7}{2}$	5-5					13096.7361	1.4[a]		
	$\frac{5}{2}$-$\frac{3}{2}$	1-1	13333.4381	0.0[a]			13096.9809	0.4		
	$\frac{5}{2}$-$\frac{3}{2}$	2-2	13334.9105	0.1			13098.4085	-1.0		
	$\frac{7}{2}$-$\frac{5}{2}$	3-3					13099.7812	0.3		
	$\frac{7}{2}$-$\frac{5}{2}$	2-1	13337.2438	0.4			13100.8257	2.1		
	$\frac{7}{2}$-$\frac{5}{2}$	5-4	13337.3196	-0.5	13293.1079	-0.1[a]	13100.9083	-0.9	13057.8598	0.3[a]
	$\frac{5}{2}$-$\frac{3}{2}$	4-3	13337.5968	-0.6	13293.3595	-0.1	13101.0858	-0.4	13058.0381	0.8
	$\frac{7}{2}$-$\frac{5}{2}$	3-2	13339.1978	-0.7	13294.9570	0.0	13102.7689	-1.2	13059.6907	-1.5
	$\frac{5}{2}$-$\frac{3}{2}$	3-2					13102.7823	1.0		
	$\frac{7}{2}$-$\frac{5}{2}$	4-3	13339.2623	0.8	13295.0203	2.5	13102.8464	-0.1	13059.7662	0.6
	$\frac{5}{2}$-$\frac{3}{2}$	3-2	13339.2623	-0.5	13295.0203	-3.6				
	$\frac{5}{2}$-$\frac{3}{2}$	2-1	13340.9177	0.2			13104.4402	0.3		
	$\frac{5}{2}$-$\frac{3}{2}$	3-3	13345.1936	-1.3			13108.7187	-1.3		
	$\frac{9}{2}$-$\frac{9}{2}$	6-6	13447.9105	1.6			13193.4592	1.0		
5-4	$\frac{11}{2}$-$\frac{9}{2}$	7-6	16656.8612	-0.2	16601.5705	0.6	16363.8308	-0.5	16309.9952	-0.7
	$\frac{11}{2}$-$\frac{9}{2}$	4-3			16601.7753	-2.1	16364.0452	-1.7		
	$\frac{13}{2}$-$\frac{11}{2}$	8-7	16657.1043	-0.5	16601.8106	0.7	16364.0687	0.2	16310.2294	-0.1
	$\frac{13}{2}$-$\frac{11}{2}$	7-6	16657.3127	-0.2	16602.0138	-0.5	16364.2793	-0.5	16310.4358	-1.3
	$\frac{13}{2}$-$\frac{11}{2}$	5-4	16657.4141	0.6	16602.1151	2.0	16364.3819	0.6	16310.5389	2.0
	$\frac{11}{2}$-$\frac{9}{2}$	6-5	16657.5204	-0.7			16364.4876	-1.2	16310.6426	-0.5
	$\frac{13}{2}$-$\frac{11}{2}$	6-5	16657.5938	0.9	16602.2880	-1.8	16364.5589	0.9	16310.7101	-1.0
	$\frac{11}{2}$-$\frac{9}{2}$	5-4	16657.7306	0.2	16602.4255	0.5	16364.6962	0.3	16310.8489	1.9
	$\frac{9}{2}$-$\frac{7}{2}$	6-5	16665.0306	-0.1	16609.7492	0.5	16370.6681	-0.8	16316.8447	3.3
	$\frac{7}{2}$-$\frac{5}{2}$	5-4	16665.1328	-0.7	16609.8519	-0.3	16370.7399	0.2	16316.9121	-0.7
	$\frac{9}{2}$-$\frac{7}{2}$	3-2	16665.2553	1.5			16370.8820	0.7		
	$\frac{7}{2}$-$\frac{5}{2}$	4-3	16665.8149	0.3			16371.4196	0.2		
	$\frac{9}{2}$-$\frac{7}{2}$	5-4	16665.9579	0.0			16371.5910	0.0		
	$\frac{7}{2}$-$\frac{5}{2}$	2-1	16666.0724	-0.8			16371.6794	2.2		
	$\frac{9}{2}$-$\frac{7}{2}$	4-3	16666.2496	0.9			16371.8778	0.1		
	$\frac{7}{2}$-$\frac{5}{2}$	3-2	16666.7953	0.2			16372.4058	0.5		

Relativistic effects on the properties of coinage metal compounds usually mean that simple periodic trends no longer apply (see, for example, Ref. (5)). One of the main results is bond contraction due to relaxation of the kinetic repulsion between the two atoms (3, 4, 14). Consequently, for a metal–halogen bond for a particular halogen atom the AuX distance is actually shorter than the corresponding AgX distance. These effects are shown in Fig. 3, which contains plots of the r_e values of CuX, AgX, and AuX (X = F, Cl, Br). It can be seen that there is a consistent decrease of ~0.08 Å in bond length in going from AgX to AuX.

NUCLEAR QUADRUPOLE COUPLING CONSTANTS

Very precise nuclear quadrupole coupling constants (NQCC) have been obtained for both nuclei, for both mole-cules. Their isotopic ratios, for both Cl and Br, should be those of the quadrupole moments of the nuclei. These ratios are given in Table 9 for the $v = 0$ and $v = 1$ vibrational states. They are indeed in excellent agreement, as anticipated. This agreement is especially important in the present work because of the extraordinary variations in the Au NQCC among the molecules, as discussed below. Extra evidence was required to assign eQq values to the nuclei, and these ratios have provided it.

The NQCC of all the nuclei show significant dependence on vibrational state. This dependence can be written in the form

$$eQq_v = eQq_e + \alpha_{eQq}(v + \tfrac{1}{2}) + \gamma_{eQq}(v + \tfrac{1}{2})^2, \qquad [9]$$

where eQq_e is the equilibrium NQCC, and α_{eQq} and γ_{eQq} are vibration–rotation correction terms. Their values, obtained

TABLE 5
Molecular Constants Calculated for AuBr in MHz[a]

Parameters	Au^{79}Br		Au^{81}Br	
	$v=0$	$v=1$	$v=0$	$v=1$
B_v	1665.996625(41)	1660.467068(77)	1636.651718(41)	1631.267772(81)
$D_{Jv} \times 10^4$	2.959(11)	2.961(18)	2.853(11)	2.863(19)
$eQq(\mathrm{Au})_v$	37.2669(14)	36.6572(78)	37.2702(16)	36.6683(80)
$eQq(\mathrm{Br})_v$	492.3271(12)	492.899(18)	411.2827(12)	411.738(18)
$C_I(\mathrm{Au}) \times 10^4$	3.86(64)	3.86[b]	3.58(66)	3.58[b]
$C_I(\mathrm{Br}) \times 10^3$	1.418(66)	1.55(28)	1.405(69)	1.43(29)

[a] Numbers in parentheses are one standard deviation in units of last significant figure.

[b] Fixed to ground state value.

from the results in Table 3 and 5, are listed in Table 10. It is clearly seen that the NQCC of Au are especially vibrational state-dependent; presumably they are very sensitive to structural variations with vibrational state. This dependence is much smaller for the halogens.

The ionic characters of the AuCl and AuBr bonds can be estimated from the halogen NQCC. If contributions from the d-orbitals of Cl and Br are neglected in the bonding orbitals, the ionic characters can be related to the coupling constants by

$$i_c = 1 + eQq_0(X)/eQq_{nl0}(X), \qquad [10]$$

where eQq_{nl0} is the NQCC for a singly occupied np_z ($n = 3$ and 4 for Cl and Br, respectively) orbitals of atomic Cl or Br [$eQq_{310}(^{35}\mathrm{Cl}) = +109.74$ MHz; $eQq_{410}(^{79}\mathrm{Br}) = -769.76$ MHz (39)]. The results are listed in Table 11 with various halide-containing diatomic species, including metal monoha-

lide species. It can be seen that both AuCl and AuBr are substantially more covalent than their Cu and Ag counterparts and their ionic characters are similar in magnitude to those of HCl and HBr. This is expected because of the high electronegativity of Au (Pauling-type 2.54) compared to the other group 11 metals (1.90 and 1.93 for Cu and Ag, respectively (42)).

The NQCC values for Au, and particularly their variation from halide to halide, are quite remarkable. The ground vibrational state NQCC values vary from -53.2387 MHz in AuF (22) to $+9.663312$ and $+37.2669$ MHz in Au^{35}Cl and Au^{79}Br, respectively. Such a variation implies that the electronic structure at Au changes significantly in going from AuF to AuBr. In an attempt to account for this, we have obtained Mulliken orbital populations from our relativistic MP2 calculations described earlier and have applied them to a simple Townes–Dailey analysis (43, 44).

TABLE 6
Equilibrium Constants Obtained for AuCl[a]

Parameters	Au^{35}Cl	Literature Values			Au^{37}Cl
		Expt.[b]	Theory[c]	Theory[d]	
B_e/MHz	3519.23798(21)	3519.20(33)	3483	3279	3357.78042(12)
α_e/MHz	16.30261(46)	16.28(27)	14.5		15.19461(14)
γ_e/MHz	0.00437(14)				0.00437[e]
r_e/Å	2.1990287(9)	2.19903(21)	2.211	2.278	2.1990283(9)
ω_e/cm^{-1}	383.61(77)	383.3018(16)	393.1	383	374.46(87)
$\omega_e x_e$/cm^{-1}	1.4569(32)	1.33	1.254		1.3878(36)
D_e/eV	3.13	3.42[f]	2.973	2.516	3.13

[a] Numbers in parentheses are one standard deviation in units of last significant figure. The uncertainty given for r_e is derived from those of the fundamental constants, rotational constants, and atomic masses.

[b] Reference (24). The value of $\omega_e x_e$ used in Ref. (24) was taken from Ref. (23).

[c] MP2 level of theory, Ref. (9).

[d] CEPA-1 method, Ref. (5).

[e] Fixed to Au^{35}Cl value.

[f] D_e was derived from the results in Ref. (24) by the same method used in the present work.

TABLE 7
Equilibrium Constants Obtained for AuBr[a]

Parameters	Au^{79}Br	Au^{81}Br
B_e/MHz	1668.761404(60)	1639.343691(61)
α_e/MHz	5.529557(87)	5.383946(91)
r_e/Å	2.318410(1)	2.318410(1)
ω_e/cm^{-1}	264.38(49)	262.16(51)
$\omega_e x_e$/cm^{-1}	0.7306(15)	0.7183(15)
D_e/eV	2.96	2.96

[a] Numbers in parentheses are one standard deviation in units of last significant figure.

The results of the Mulliken population analysis are listed in Table 12. They show a significant increase in the populations of the Au σ-orbitals ($5d_\sigma$, $6s$, and $6p_\sigma$), and a slight increase of the $6p_\pi$ orbital, in going from AuF to AuBr. This trend follows the decrease in electronegativity in going from F to Br. The populations were applied to the following modified Townes–Dailey equation (43, 44)

$$eQq = eQq_{610}(n_{6p_\sigma} - 0.5n_{6p_\pi})$$
$$+ eQq_{520}(n_{5d_\sigma} + 0.5n_{5p_\pi} - n_{5d_\delta}), \quad [11]$$

where n are the total Mulliken populations of the orbitals indicated, and eQq_{610} and eQq_{520} have been estimated from (13, 28)

$$eQq_{nl0} = -2.353 \frac{2l(l + 1)}{(2l + 3)(2l - 1)} Q \left\langle \left(\frac{a_0}{r}\right)^{-3} \right\rangle. \quad [12]$$

Using the values for $\langle r^{-3} \rangle = 5.19a_0^{-3}$ and $12.58a_0^{-3}$ for the $6p$ (45) and $5d$ (18) orbitals, respectively, and $Q = 54.7$ fm^2 (46), values of $eQq_{610} = -534$ MHz and $eQq_{520} = -925$ MHz are obtained. When these are used in Eq. [11], the resulting Au eQq values are +213, +140, and +12 MHz for AuF, AuCl, and AuBr, respectively, nowhere near the experi-

TABLE 8
Calculated Molecular Constants of AuF, AuCl, and AuBr

	AuF	AuCl	AuBr
r_e/Å MP2	1.918	2.200	2.337
Observed	1.918449[a]	2.1990287	2.3184102
B_e/MHz MP2	7931	3515	1642
Observed	7896.81976[a]	3519.23798	1668.761404
ω_e/cm^{-1} MP2	555.1	391.8	273.1
Observed		383.3018[b]	264.38[c]

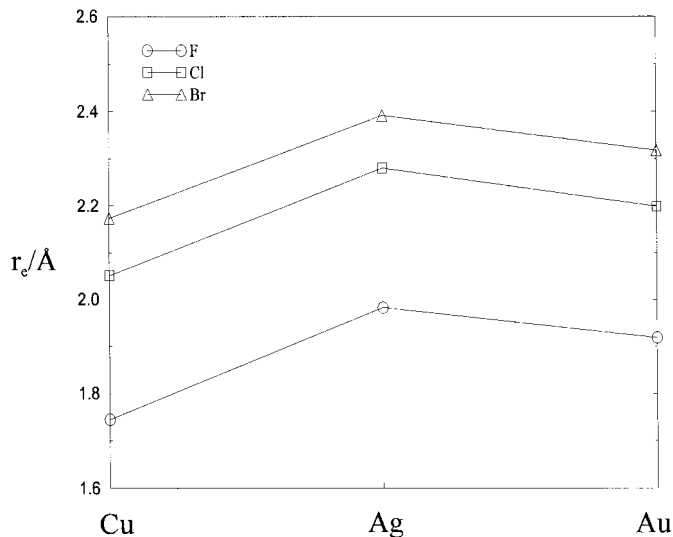[a] Reference (22).
[b] Reference (24).
[c] This work from Eq. (6).

FIG. 3. Equilibrium bond lengths of CuX, AgX, and AuX (X = F, Cl, Br).

mental results. Once again, this simple theory has failed to account for transition metal NQCC values (21). Particularly noteworthy is the failure to reproduce the variations in sign.

The quadrupole moments of the elements are generally not very well determined. One way of improving their values is by using the observed nuclear quadrupole coupling constant in atoms, molecules, or solids in conjunction with a calculated or estimated value of the electric field gradient (EFG). Calculation of EFG has in recent years improved considerably, so much so that quadrupole moments can be estimated with an accuracy (if accurate nuclear quadrupole constants are available) of ~1%. Pernpointer et al. (47) have performed Douglas–Kroll coupled cluster calculations for the EFG of group 11 metal chlorides (CuCl, AgCl, AuCl) using the point-charge nuclear quadrupole moment (PCNQM) method. The quadrupole moment and the electric field gradient are related through the equation

$$Q = -\frac{eQq}{2.349647q}, \quad [13]$$

TABLE 9
Ratios of eQq for Cl and Br in AuCl and AuBr[a]

	$v=0$	$v=1$	Equil.	Lit.[b]
$\dfrac{eQq(^{35}Cl)}{eQq(^{37}Cl)}$	1.268886(28)	1.269001(44)	1.268804(66)	1.2688773(15)[c]
$\dfrac{eQq(^{79}Br)}{eQq(^{81}Br)}$	1.1970527(45)	1.197118(68)	1.197019(68)	1.197050(1)[d]

[a] Numbers in parentheses are one standard deviation in units of the last significant figure.
[b] The literature values are the ratios of the nuclear quadrupole moments.
[c] Reference (40).
[d] Reference (41).

TABLE 10

Equilibrium eQq Values (in MHz) for AuF, AuCl, and AuBr[a]

	eQq_e	α_{eQq}	γ_{eQq}
^{197}Au in AuF[b]	-52.965(12)	-0.5378(95)	
^{197}Au in Au^{35}Cl	10.0107(18)	-0.7615(37)	0.0127(13)
^{35}Cl in Au^{35}Cl	-61.9527(23)	-0.0885(48)	
^{197}Au in Au^{37}Cl	10.0106(34)	-0.7447(30)	0.0127[c]
^{37}Cl in Au^{37}Cl	-48.8276(18)	-0.0633(16)	
^{197}Au in Au^{79}Br	37.5717(80)	-0.6097(79)	
^{79}Br in Au^{79}Br	492.041(18)	0.572(18)	
^{197}Au in Au^{81}Br	37.5712(84)	-0.6019(82)	
^{81}Br in Au^{81}Br	411.055(18)	0.455(18)	

[a] Numbers in parentheses are one standard deviation in units of the last significant figure.

[b] Reference (22).

[c] Fixed to Au^{35}Cl value.

where Q is the quadrupole moment in square femtometres^2, eQq is the nuclear quadrupole coupling constant (NQCC) in megahertz, and q is the electric field gradient in atomic units. For CuCl, Pernpointer et al. (47) calculated q(Cu) = −0.3467 and q(Cl) = +1.7058 a.u., which using Q(Cu) = −21.1 and Q(Cl) = −8.11 fm^2 (46) in the above equation give eQq(Cu) = +17.18 and eQq(Cl) = −32.505 MHz, which are in excellent agreement with the experimental values of eQq_0(Cu) = +16.169 and eQq_0(Cl) = −32.127 MHz (48). For AuCl, they calculated q(Au) = +0.5869 and q(Cl) = +3.1854 a.u., which give eQq(Au) = +75.43 and eQq(Cl) = −60.69 MHz. The result for chlorine is again in very good agreement with the experimental value eQq_e = −61.9527 MHz; however, their result for Au (although half of that found using the simple Townes–Dailey approach) is considerably higher than the experimental value of eQq_e(Au) = +10.0107 MHz.

TABLE 11

Ionicity of Some Selected Halide-Containing Diatomic Species

	$i_c\%$ Cl	$i_c\%$ Br
Cu	0.71	0.66
Ag	0.66	0.60
Au	0.43	0.36
H	0.38	0.31
Y	0.99	0.98
Na	0.95	0.92
In	0.87	0.85

TABLE 12

Mulliken Population Analysis for AuF, AuCl, and AuBr

Molecule	n_{5d_σ}	n_{5d_π}	n_{5d_δ}	n_{6s}	n_{6p_σ}	n_{6p_π}
AuF	1.78	3.98	4.00	0.38	0.04	0.08
AuCl	1.84	3.97	4.00	0.54	0.09	0.10
AuBr	1.92	4.00	4.00	0.73	0.17	0.11

CONCLUSIONS

The microwave spectra of AuCl and AuBr have been measured for the first time to produce rotational and centrifugal distortion constants, along with nuclear quadrupole coupling constants. The equilibrium bond distance and harmonic vibrational frequency of AuCl and AuBr have been determined along with their dissociation energies. From the halide nuclear quadrupole constants, the AuCl and AuBr bonds have been shown to be predominantly covalent in nature. The changes in the gold nuclear quadrupole coupling constant from one halogen to the next indicate substantial changes in the electronic structure at gold. The simple approach of using orbital populations with the Townes–Dailey equation in estimating the nuclear quadrupole coupling constant of gold could not reproduce the observed values or even the general trends in going from one halide to the next; even recent sophisticated ab initio calculations have some difficulty making accurate predictions.

REFERENCES

1. P. Jeffrey Hay, W. R. Wadt, L. R. Kahn, and F. W. Bobrowicz, J. Chem. Phys. **69,** 984–997 (1978).
2. H. Basch and S. Topiol, J. Chem. Phys. **71,** 802–814 (1979).
3. T. Ziegler, J. G. Snijders, and E. J. Baerends, Chem. Phys. Lett. **75,** 1–4 (1980).
4. T. Ziegler, J. G. Snijders, and E. J. Baerends, J. Chem. Phys. **74,** 1271–1284 (1981).
5. P. Schwerdtfeger, M. Dolg, W. H. E. Schwarz, G. A. Bowmaker, and P. D. W. Boyd, J. Chem. Phys. **91,** 1762–1774 (1989).
6. P. Schwerdtfeger, P. D. W. Boyd, A. K. Burrell, W. T. Robinson, and M. J. Taylor, Inorg. Chem. **29,** 3593–3607 (1990).
7. O. D. Häberlen and N. Rösch, Chem. Phys. Lett. **199,** 491–496 (1992).
8. P. Schwerdtfeger, J. S. McFeaters, R. L. Stephens, M. J. Liddell, M. Dolg, and B. A. Hess, Chem. Phys. Lett. **218,** 362–366 (1994).
9. P. Schwerdtfeger, Mol. Phys. **86,** 359–368 (1995).
10. P. Schwerdtfeger, J. S. McFeaters, M. J. Liddell, J. Hrušák, and H. Schwarz, J. Chem. Phys. **103,** 245–252 (1995).
11. V. A. Nasluzov and N. Rösch, Chem. Phys. **210,** 913–925 (1996).
12. M. Iliaš, P. Furdík, and M. Urban, J. Phys. Chem. A **102,** 5263–5268 (1998).
13. C. van Wüllen, J. Chem. Phys. **109,** 392–399 (1998).
14. P. Pyykkö, Chem. Rev. **88,** 563–594 (1988) [and references therein].
15. R. J. Puddephatt, "The Chemistry of Gold," Elsevier, New York, 1978.
16. [See, for example, P. Machmer, Inorg. Nucl. Chem. **30,** 2627–2634 (1968)].
17. (a) C. A. McAuliffe, R. V. Parish, and P. D. Randell, J. Chem. Soc. Dalton 1426–1430 (1977); (b) P. G. Jones and A. F. Williams, J. Chem. Soc. Dalton 1430–1434 (1977); (c) P. G. Jones, A. G. Maddock, M. J. Mays,

M. M. Muir, and A. F. Williams, *J. Chem. Soc. Dalton* 1434–1439 (1977); (d) D. Guenzburger and D. E. Ellis, *Phys. Rev. B* **22,** 4203–4214 (1980).

18. D. M. S. Esquivel, D. Guenzburger, and J. Danon, *Phys. Rev. B: Condens. Matter* **19,** 1357–1364 (1979).

19. K. A. Walker and M. C. L. Gerry, *J. Mol. Spectrosc.* **198,** 183–185 (1999).

20. K. A. Walker and M. C. L. Gerry, *J. Chem. Phys.* **109,** 5439–5445 (1998).

21. W. Lin, S. A. Beaton, C. J. Evans, and M. C. L. Gerry, *J. Mol. Spectrosc.* **199,** 275–283 (2000).

22. C. J. Evans and M. C. L. Gerry, *J. Amer. Chem. Soc.* **122,** 1560–1561 (2000).

23. W. F. C. Ferguson, *Phys. Rev.* **31,** 969–972 (1928).

24. L. C. O'Brien, A. L. Elliot, and M. Dulick, *J. Mol. Spectrosc.* **194,** 124–127 (1999).

25. T. J. Balle and W. H. Flygare, *Rev. Sci. Instrum.* **52,** 33–45 (1981).

26. Y. Xu, W. Jäger, and M. C. L. Gerry, *J. Mol. Spectrosc.* **151,** 206–216 (1992).

27. K. A. Walker and M. C. L. Gerry, *J. Mol. Spectrosc.* **182,** 178–183 (1997).

28. S. A. Beaton and M. C. L. Gerry, *J. Chem. Phys.* **110,** 10715–10724 (1999).

29. C. Møller and M. S. Plesset, *Phys. Rev.* **46,** 618–622 (1934).

30. M. J. Frisch, G. W. Trucks, H. B. Schlegel, G. E. Scuseria, M. A. Robb, J. R. Cheeseman, V. G. Zakrzewski, J. A. Montgomery, R. E. Stratmann, J. C. Burant, S. Dapprich, J. M. Millam, A. D. Daniels, K. N. Rudin, M. C. Strain, O. Farkas, J. Tomasi, V. Barone, M. Cossi, R. Cammi, B. Mennucci, C. Pomelli, C. Adamo, S. Clifford, J. Ochterski, G. A. Petersson, P. Y. Ayala, Q. Cui, K. Morokuma, D. K. Malick, A. D. Rabuck, K. Raghavachari, J. B. Foresman, J. Cioslowski, J. V. Ortiz, B. B. Stefanov, G. Liu, A. Liashenko, P. Piskorz, I. Komaromi, R. Gomperts, R. L. Martin, D. J. Fox, T. Keith, M. A. Al-Lahma, C. Y. Peng, A. Nanayakkara, C. Gonzalez, M. Challacombe, P. M. W. Gill, B. G. Johnson, W. Chen, M. W. Wong, J. L. Andres, M. Head-Gordon, E. S. Replogle, and J. A. Pople, "GAUSSIAN 98, Revision A.6," Gaussian, Inc., Pittsburgh, PA, 1998.

31. P. Schwerdtfeger, *Chem. Phys. Lett.* **183,** 457–463 (1991).

32. R. A. Kendall, T. H. Dunning, Jr., and R. J. Harrison, *J. Chem. Phys.* **96,** 6796–6806 (1992).

33. D. E. Woon and T. H. Dunning, Jr., *J. Chem. Phys.* **98,** 1358–1371 (1993).

34. H. M. Pickett, *J. Mol. Spectrosc.* **148,** 371–377 (1991).

35. L. C. Krisher and W. G. Norris, *J. Chem. Phys.* **44,** 391–394 (1966).

36. L. C. Krisher and W. G. Norris, *J. Chem. Phys.* **44,** 974–976 (1966).

37. A. Kratzer, *Z. Phys.* **3,** 289 (1920).

38. C. L. Pekeris, *Phys. Rev.* **45,** 98–103 (1934).

39. W. Gordy and R. L. Cook, "Microwave Molecular Spectra," Wiley, New York, 1984.

40. F. J. Lovas and E. Tiemann, *J. Phys. Chem. Ref. Data* **3,** 609–769 (1974).

41. A. C. Legon and J. C. Thorn, *Chem. Phys. Lett.* **215,** 554–560 (1993).

42. J. E. Huheey, "Inorganic Chemistry," 3rd ed., Harper and Row, New York, 1983.

43. C. H. Townes and B. P. Dailey, *J. Chem. Phys.* **17,** 782–796 (1949).

44. T. L. Brown, *Acc. Chem. Res.* **1,** 408 (1974).

45. C. E. Moore, *Natl. Stand. Ref. Data Ser. (U.S. Natl. Bur. Stand.)* **35** (1971).

46. I. Mills, T. Cvitaš, K. Homann, N. Kallay, and K. Kuchitsu, "Quantities, Units, and Symbols in Physical Chemistry," 2nd ed., Blackwell Scientific Publications, Oxford, 1993.

47. M. Pernpointer, P. Schwerdtfeger, and B. A. Hess, *Int. J. Quantum Chem.* **76,** 371–384 (2000).

48. R. J. Low, T. D. Varberg, J. P. Connelly, A. R. Auty, B. J. Howard, and J. M. Brown, *J. Mol. Spectrosc.* **161,** 499–510 (1993).